ORIGINAL RESEARCH

American Society of Plant Biologists · Cultivating a better future through plant biology research

S·E·B SOCIETY FOR EXPERIMENTAL BIOLOGY

WILEY

Plasticity and the role of mass-scaling in allocation, morphology, and anatomical trait responses to above- and belowground resource limitation in cultivated sunflower (*Helianthus annuus* L.)

Yan Wang[1,2] (iD) | Lisa A. Donovan[2] | Andries A. Temme[2] (iD)

[1]College of Forestry, Shandong Agriculture University, Taian, Shandong, China

[2]Department of Plant Biology, Franklin College of Arts and Sciences, The University of Georgia, Athens, GA, USA

Correspondence
Andries A. Temme, Department of Plant Biology, Franklin College of Arts and Sciences, The University of Georgia, Athens, GA, USA.
Email: atemme@uga.edu

Abstract

In the face of resource limitations, plants show plasticity in multiple trait categories, including biomass allocation, morphology, and anatomy, yet inevitably also grow less. The extent to which passive mass-scaling plays a role in trait responses that contribute to increased potential for resource acquisition is poorly understood. Here, we assessed the role of mass-scaling on the direction, magnitude, and coordination of trait plasticity to light and/or nutrient limitation in cultivated sunflower (*Helianthus annuus*). We grew seedlings of 10 sunflower genotypes for 3 weeks in a factorial of light (50% shade) and nutrient (10% supply) limitation in the greenhouse and measured a suite of allocational, morphological, and anatomical traits for leaves, stems, fine roots, and tap roots. Under resource limitation, plants were smaller and more biomass was allocated to the organ capturing the most limiting resource, as expected. Traits varied in the magnitude of plasticity and the extent to which the observed response was passive (scaled with plant mass) and/or had an additional active component. None of the allocational responses were primarily passive. Plastic changes to specific leaf area and specific root length were primarily active, and adjusted toward more acquisitive trait values under light and nutrient limitation, respectively. For many traits, the observed response was a mixture of active and passive components, and for some traits, the active adjustment was antagonistic to the direction of passive adjustment, for example, stem height, and tap root and stem theoretical hydraulic conductance. Passive scaling with size played a major role in the coordinated response to light, but correcting for mass clarified that the active responses to both limitations were more similar in magnitude, although still resource and organ specific. Our results demonstrate that both passive plasticity and active plasticity can contribute to increased uptake capacity for limiting resources in a manner that is resource, organ, and trait specific. Indeed, passive adjustments (scaling with mass) of traits due to resource stress extend well beyond just mass allocation traits. For a full

understanding of plants' response to environmental stress, both passive and active plasticity need to be taken into account.

1 | INTRODUCTION

The extent of plant trait adjustment in response to a changed environment is generally considered as the plant's phenotypic plasticity (Nicotra et al., 2010; Valladares et al., 2007). According to theory, this plasticity serves to optimize/maximize the uptake of the most limiting resource (Bloom et al., 1985; Gedroc et al., 1996; Poorter et al., 2012; Shipley & Meziane, 2002). For example, increased mass allocation to leaves under shade, and to roots under nutrient limitation, alleviates some of the stress caused by the resource limitation (Shipley & Meziane, 2002; Sugiura & Tateno, 2011). However, plants are inevitably smaller under resource stress, raising the question of the role of mass-scaling in individual and coordinated trait shifts in response to resource limitation (McConnaughay & Coleman, 1999; Osnas et al., 2013; Poorter et al., 2012; Reich, 2014; Shipley & Meziane, 2002; Weiner, 2004).

There is a long tradition of investigating mass-based scaling of biomass allocation to different plant parts (Weiner, 2004). Generally, smaller plants allocate proportionally more mass to leaves than to roots (Poorter et al., 2012). Trait responses that scale with mass, which have been variously called allometric scaling, "passive" plasticity, or "apparent" plasticity, could predispose the plant to align its traits with resource availability and demand (McConnaughay & Coleman, 1999; Nicotra et al., 2010; Poorter et al., 2012; van Kleunen & Fisher, 2005; Weiner, 2004). However, there is evidence that additional "active" or "true" plasticity in biomass allocation can further increase the capacity for acquiring the most limiting resource (McConnaughay & Coleman, 1999; Poorter et al., 2012; Shipley & Meziane, 2002). There is also evidence of active plasticity in other traits related to resource uptake. For example, under low light conditions, greater plant height and greater specific leaf area for a given plant mass aid in light uptake (Freschet et al., 2015, 2018; Reich, 2018; Rice & Bazzaz, 1989). Thus, both passive and active trait adjustments combine in the realized response to resource stress.

The role of passive and active contributions to observed responses can be investigated by including analyses that correct responses for plant size (Poorter et al., 2012; Reich, 2018). In this framework, passive adjustments in traits associated with size cannot be a priori regarded as or ruled out as adaptive (Nicotra et al., 2010; Poorter et al., 2012, 2019). If trait responses that are consistent with greater ability to take up the most limiting resource have both passive and active components, it will be important to consider both the magnitude and alignment of both components when evaluating evidence for functional and putatively adaptive responses.

Among plant traits, anatomical traits are often overlooked due to time and budget constraints. However, variation in anatomical traits underlies or contributes to variation in morphological and physiological traits that have received more attention (John et al., 2017; Kong et al., 2014; Scoffoni et al., 2015). For example, palisade parenchyma thickness is positively correlated with leaf thickness (Catoni et al., 2015) and photosynthetic rate (Chatelet et al., 2013). Additionally, a thicker cortex could provide a relative larger site for mycorrhizal infection and higher resource uptake in thicker roots, especially for the arbuscular mycorrhiza (Kong et al., 2014). Root cortex thickness, due to the size of cortical cells (Eissenstat & Achor, 1999), strongly affects fine root diameter (Gu et al., 2014; Guo et al., 2008), and a wider stele and/or xylem conduit greatly affects hydraulic conductivity (McElrone et al., 2004; Rico et al., 2013; Tyree & Ewers, 1991). Thus, exploring how passive and active responses in anatomical traits align with those of other traits will enhance our understanding of how plants adjust to changing environmental conditions from tissue, to organ, to architecture.

Across species, plant functional traits are thought to form a spectrum of resource use strategies from fast to slow (Díaz et al., 2016; Fortunel et al., 2012; Reich, 2014; Wright et al., 2004). The "whole plant economic spectrum" suggests that values of traits related to resource use, including mass allocation, morphology, and transport, should be coordinated across all organs and resources, with more resource-conservative traits associated with adaptation to light- and nutrient-limited habitats (Reich, 2014). For closely related species, there is mixed evidence of correlated evolution among some traits related to resource acquisition and processing (Bowsher et al., 2016; Mason & Donovan, 2015; Medeiros et al., 2017; Muir et al., 2017; Pilote & Donovan, 2016). However, much remains unclear about how the coordinated traits across "whole plant economic spectrum" relate to trait plasticity in response to resource limitations (Agrawal, 2020; Anderegg et al., 2018; Reich, 2014). Thus, it is interesting to assess the coordination of responses across organs and a broad range of traits in terms of the role of passive and active plasticity.

To add to our understanding of plant responses to resource limitation, we examined trait responses to light and nutrient limitation of traits across different trait categories (biomass allocation, morphology, and anatomy) and organs (leaf, stem, and root) in cultivated sunflower. Prior research has shown strong plastic responses to resource limitation and other environmental factors in *H. annuus* (Bowsher et al., 2017; Donovan et al., 2014; Masalia et al., 2018; Rico et al., 2013; Temme et al., 2019). Specifically, we sought to answer the following questions:

1. How do mass allocation, organ morphology, and anatomy change with above- and belowground resource limitation, and what role does size scaling of traits play in this?

2. How do traits compare for magnitude of plasticity and what role does size scaling of traits play in this?

3. Do traits show a coordinated shift due to resource limitation across all organs and what role does size scaling of traits play in this?

2 | MATERIAL AND METHODS

2.1 | Experimental design

To address these questions, we selected a set of 10 cultivated sunflower genotypes (Table S1), varying broadly in biomass based on prior work, from a larger diversity panel used for genomic dissection of traits (Mandel et al., 2011; Masalia et al., 2018; Nambeesan et al., 2015). We conducted a factorial design of two nutrient treatments (rich and poor) and two light treatments (sun and shade) at the Botany greenhouses of The University of Georgia, Athens GA, USA, in March 2018. Achenes were sown in seedling trays and allowed to grow for 7 days, after which each seedling was transplanted to 5 liter (1.3 gallon) pot filled with a 3:1 sand:calcinated clay mixture (Turface MVP, Turface Athletics). Pots were arranged in a split plot design of six replicate blocks. The light treatment was applied as the whole-plot factor, with two subplots in each plot randomly assigned to unshaded or 50% shade generated with high-density woven polyethylene cloth (Figure S1). Within each subplot, two pots of each genotype were randomly distributed and supplied with either 40 g or 4 g fertilizer (Osmocote Plus 15-9-12 with micronutrients, Scotts, Marysville, OH, USA), totaling 240 pots (plants). Greenhouse temperature controls were set to maintain 18–24°C, and natural sunlight was supplemented with sodium halide lighting (20–25 μ mol/m^2 s^{-1}) to maintain a 15/9-hr photoperiod.

2.2 | Plant harvest and trait measurements

Plants were harvested 3 weeks after transplanting (4 weeks after germination). At harvest, stem height (ST-Hgt, from soil surface to top of apical meristem) and stem diameter (ST-Dia, midway between cotyledons and first leaf pair) were measured. Plants were separated into root, leaf (including cotyledons), and stem (including bud if present—rarely) for biomass and other measurements. We assigned all measured traits to one of the three categories (allocational, morphological, and anatomical) in order to compare the relative magnitude of adjustments to these broad categories. While we believe our assignment of traits to categories is defensible, we acknowledge that this is somewhat arbitrary and that different groupings could influence the results associated with comparisons among categories.

Each replicate plant was sampled for leaf, stem, and root tissue for anatomical traits. One recently matured, fully expanded leaf was sampled for a 1 × 0.5 cm rectangle cut out of the leaf center.

The stem was sampled for a 5 mm length segment centered between the cotyledon and the first leaf pair. The root was sampled for both tap root and fine root tissue. For the tap root, a 1 cm segment was cut 4 cm below the root/stem junction. For a single lateral root attached to the tap root near to the root/stem junction with an intact root tip, a 1 cm fine root segment was cut 2 cm from the apex of the root. All tissue subsamples were weighed for fresh mass and then fixed in formalin–acetic acid–alcohol solution, FAA (50% ethanol (95%), 5% glacial acetic acid, 10% formaldehyde (37%), and 35% distilled water.

Fixed subsamples were processed for anatomy at the University of Georgia Veterinary Histology Laboratory. Each sample was embedded and gradually infiltrated with paraffin, sliced with a sledge microtome, mounted to a slide, and stained with safranin and fast green dye. Slides were imaged with a camera-mounted Zeiss light microscope using ZEN software (Carl Zeiss Microscopy). For leaf, stem, and fine and tap roots, the dimensions of anatomical features were traced using Motic Images Advanced 3.2 software (Motic Corporation). The organ dimensions included leaf thickness (LF-Th), fine root diameter (FR-Dia), and tap root diameter (TR-Dia). The tissue dimensions included leaf palisade thickness (LF-PT), leaf spongy thickness (LF-ST), stem cortex thickness (ST-CT), stem xylem thickness (ST-XT), tap root cortex thickness (TR-CT), tap root stele diameter (TR-SDia), fine root cortex thickness (FR-CT), and fine root stele diameter (FR-SDia). The theoretical hydraulic conductivity (Ks, kg·s^{-1}·m^{-1}·MPa^{-1}) per vascular area for leaf (LF-Ks), stem (ST-Ks), fine root (FR-Ks), and tap root (TR-Ks) tissue was calculated (Sperry et al., 2006), based on the Hagen-Poiseuille equation (Tyree & Ewers, 1991): $ks = \left(\pi \rho / 128 \eta A_w \right) \sum_{i=1}^{n} d_i^4$, where ρ is the density of water (988.3 kg·m^{-3} at 20°C); η is the viscosity of water (1.002 × 10^{-9} MPa·s at 20°C); A_w is the stele (vascular) cross-section area; d is the diameter of the ith vessel; and n is the number of conduits in the xylem.

After anatomical samples were collected, the remaining plant material was used to determine morphological traits. The leaf, stem, and fine and tap roots for each plant were weighed for fresh mass. Root tissue, stem tissue, and the most recently fully expanded leaf were scanned at 300 dpi with an Epson Expression 1680 scanner (Seiko Epson Corporation) and saved as a TIF image. Total root length and volume of scanned fine root, tap root and stem, as well as leaf area were measured using WinRhizo (v. 2002c, Regent Instruments). Subsequently, the leaf, stem, and fine roots and tap roots were dried at 60°C for 48 hr and weighed. Specific leaf area (LF-SLA, cm^2·g^{-1}) was calculated as the ratio of leaf area to leaf dry mass. Specific root length (m·g^{-1}) was calculated as the ratio of root length to root dry mass for the tap root and fine roots (TR-SRL and FR-SRL, respectively). Tissue density (g·cm^{-3}) was calculated as the ratio of dry mass to volume for stem, tap toot, and fine roots (ST-Den, TR-Den, and FR-Den, respectively). Leaf dry matter content, measured as leaf dry mass divided by leaf fresh mass, was used as a proxy for leaf tissue density (LF-Den) (Kramer-Walter et al., 2016; Wilson et al., 1999).

For allocational traits, total plant dry mass was calculated as the sum of all plant parts, including the subsamples for anatomical

and morphological traits. The fresh biomass of subsamples for anatomical analysis was converted to dry biomass based on the ratio of fresh/dry biomass for the morphological traits. The mass fractions for each tissue were calculated as proportions of total plant dry mass $(g \cdot g^{-1})$.

2.3 | Data analysis

The statistical analysis for the phenotypic data was performed using R v3.5.1 (R Core Team). To obtain genotype means from our split plot design, a mixed effects model was fitted using the package *lme4* (Bates et al., 2018) with genotype, light and nutrient levels, and all their interactions as fixed effects and light treatment within block as random factor. Least-square (LS) means of all trait values without random factor were estimated from this model using the R package *emmeans* (Lenth et al., 2018). To test the effect of genotype and treatment on measured traits, we fitted a less expansive mixed effects model with genotype, light, and nutrient level as well as the interaction between light and nutrient levels as fixed effects (following Freschet et al., 2018) and light treatment within block as random factor. From this model, fixed effects were then tested using a Wald Chi-square test in a type III ANONA using the package *car* (Fox et al., 2018). As we were interested in the interactive effects among genotype, light, and nutrient supply on the proportional changes in functional traits, rather than on their absolute changes, we performed all analyses on log-transformed data (Freschet et al., 2015). For each trait, differences among treatments were tested using Tukey's HSD ($p = .05$) corrected for multiple comparisons. We then estimated the influence of plant size on the significance of nutrient and light limitation effects on traits by adding (log-transformed) plant biomass as a fixed factor to both models and recalculating means and significance (Ryser & Eek, 2000; Wahl et al., 2001).

To quantify the plastic response of each trait to each resource limitation treatment, we calculated the relative distance plasticity index (RDPI, Valladares et al., 2006, Scoffoni et al., 2015) as $(x'_i - x_i) / (x'_i + x_i)$, where x_i and x'_i are the mean trait values of genotypes grown under control (high-light and high-nutrient) and resource-limited condition, respectively. Additionally, the RDPI for each trait in each resource limitation treatment was recalculated after correcting for plant size (total biomass). Significant values of RDPI (difference from zero, no plasticity) were determined using *t* test on genotype averages.

To determine major axes of variation across multiple traits and identify whether there were concerted trait adjustments to limitation in above- or belowground resources, we conducted a principal component analysis (PCA) on the trait data before and after correcting for size. Differences between treatments were tested using Bonferroni-corrected, Hotelling's *t* test on the first two principal components. Data visualizations were made using *ggplot2* (Wickham et al., 2018).

3 | RESULTS

3.1 | How do plant mass allocation, organ morphology, and anatomy respond to above- and belowground resource limitation, and what role does size scaling of traits play in this?

Across all genotypes, total plant biomass decreased substantially in response to light and nutrient limitation (Figure 1 and Table 1). The biomass response to light limitation (54.7% decline) was stronger than the response to the nutrient limitation (24.7% decline), and there was no interaction of light and nutrient limitation on biomass when combined (67.1%% decline). Of the 31 allocational, morphological, and anatomical traits measured, all but two responded to at least one resource limitation (Table S2). Responses to light limitation were more prevalent than responses to nutrient limitation, and there were relatively few interactive effects of combined light and nutrient limitation.

For allocational traits, resource limitations affected all six traits, but traits were affected in contrasting ways by light and nutrient limitation. The RatioLF-FRmass (ratio of leaf mass to fine root mass) increased under light limitation due to increased LF-MF (leaf mass fraction) and decreased FR-MF (fine root mass fraction) (Figure 2b–d and Table 1). Conversely, RatioLF-FRmass decreased under nutrient limitation, due to decreased LF-MF and increased FR-MF (Figure 2f). A significant interaction of light and nutrient limitation was found for LF-MF, ST-MF (stem mass fraction), FR-MF, and RatioLF-FRmass. The RatioSLA-SRL (ratio of LF-SLA (specific leaf area) to FR-SRL (fine root-specific root length)), which
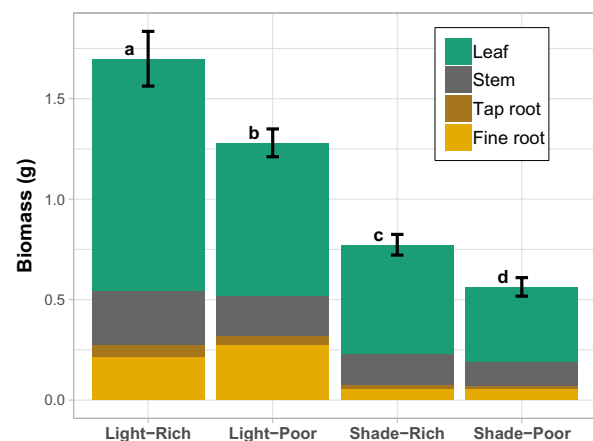
FIGURE 1 Biomass and mass allocation of leaf, stem, tap root, and fine root tissue across a factorial of light and nutrient limitation. Light/shade, direct sun versus 50% shade. Rich/poor, high nutrients versus 10% nutrient concentration. Whole plant biomass (mean ± SE) of 10 genotypes (estimated marginal mean from the ANOVA, based on 5–6 replicates per genotype) stacked by average tissue contribution. Different lower-case letters represent significant ($p < .05$) Tukey's post hoc differences between treatments for whole plant biomass

TABLE 1 Trait response to a factorial of light and nutrient limitation. Light versus shade designates direct sun versus 50% shade treatment

| Category	Treatment response	Trait	Unit	Abbreviation	Light-Rich	Light-poor	Shade-rich	Shade-poor	w/o biomass G	w/o biomass L	w/o biomass N	w/o biomass L×N	Incl. biomass Mass	Incl. biomass G	Incl. biomass MxG	Incl. biomass L	Incl. biomass N	Incl. biomass L×N	Change with mass
Allocation	Passive & active	Total Biomass	g		1.70 ± 0.14^{a}	1.28 ± 0.07^{b}	0.77 ± 0.05^{c}	0.56 ± 0.05^{d}	**	**	**	**	n/a	n/a	n/a	n/a	n/a	n/a	n/a
		Leaf mass fraction	$g \cdot g^{-1}$	LF-MF	0.68 ± 0.006^{a}	0.59 ± 0.001^{b}	0.70 ± 0.01^{c}	0.66 ± 0.01^{d}	**	**	**	**	***	***	***	***	***	***	L(*) to (ns)
		Ratio of leaf mass fine root mass	$g \cdot g^{-1}$	RatioLF-FRmass	5.58 ± 0.33^{a}	2.93 ± 0.22^{b}	9.96 ± 0.65^{c}	6.58 ± 0.40^{a}	**	**	**	**	***	***	***	***	***	***	LxN(*) to (ns)
		Ratio of leaf SLA and fine root SRL		RatioSLA-SRL	1.30 ± 0.07^{ab}	1.13 ± 0.06^{b}	1.50 ± 0.11^{a}	1.23 ± 0.04^{b}	**	*	*	*		***		*			N(*) to (ns)
	Active	Stem mass fraction	$g \cdot g^{-1}$	ST-MF	0.16 ± 0.009^{a}	0.16 ± 0.009^{a}	0.20 ± 0.001^{b}	0.21 ± 0.02^{c}	**	**	**	*		***	**	***	**	**	
		Fine root mass fraction	$g \cdot g^{-1}$	FR-MF	0.13 ± 0.007^{a}	0.21 ± 0.001^{b}	0.074 ± 0.004^{c}	0.10 ± 0.007^{d}	**	**	**	**		***	***	***	***	***	
		Tap root mass fraction	$g \cdot g^{-1}$	TR-MF	0.04 ± 0.002^{a}	0.04 ± 0.003^{a}	0.027 ± 0.002^{b}	0.03 ± 0.002^{b}	**	*				***		***		*	
Morphology	Passive	Fine root tissue density	$g \cdot cm^{-3}$	FR-Den	0.033 ± 0.002^{a}	0.033 ± 0.001^{a}	0.027 ± 0.002^{b}	0.028 ± 0.001^{ab}	**	**				***					L(*) to (ns)
		Tap root specific root length	$m \cdot g^{-1}$	TR-SRL	4.46 ± 0.43^{a}	5.04 ± 0.56^{ab}	7.35 ± 0.90^{b}	10.51 ± 2.06^{c}	**	**			*	*					L(*) to (ns)
	Passive & active	Stem Height	cm	ST-Hgt	14.62 ± 0.82^{a}	14.33 ± 0.93^{a}	16.75 ± 1.11^{b}	16.43 ± 1.64^{b}	**	**			***	***		***	*		N(ns) to (*)
		Stem diameter	mm	ST-Dia	5.23 ± 0.18^{a}	4.65 ± 0.10^{b}	4.30 ± 0.13^{b}	3.88 ± 0.11^{c}	**	**	**		***	***	***		***	***	L(*) to LxN(*)
		Tap root tissue density	$g \cdot cm^{-3}$	TR-Den	0.037 ± 0.002^{a}	0.043 ± 0.002^{b}	0.033 ± 0.002^{a}	0.033 ± 0.002^{a}	**	**	**	*		***	*		***	*	L(*) to (ns)
		Tap root diameter	μm	TR-Dia	1337.49 ± 62.57^{a}	1228.76 ± 59.19^{a}	937.87 ± 42.74^{b}	900.58 ± 36.41^{b}	**	**			**	***	*			*	L(*) to LxN(*)
	Active	Leaf thickness	μm	LF-Th	257.71 ± 8.38^{a}	248.87 ± 7.23^{a}	228.86 ± 4.75^{b}	227.24 ± 6.37^{b}	**	**			*	***		***			
		Leaf dry mass content	$mg \cdot g^{-1}$	LF-Den	102.95 ± 2.66^{a}	106.92 ± 2.55^{a}	87.33 ± 2.78^{b}	90.91 ± 2.69^{b}	**	**				***		***			
		Leaf specific leaf area	$cm^2 \cdot g^{-1}$	LF-SLA	349.53 ± 11.04^{a}	362.46 ± 6.47^{a}	487.72 ± 8.96^{b}	493.42 ± 18.32^{b}	**	**			**	***	**	***			
		Stem tissue density	$g \cdot cm^{-3}$	ST-Den	0.039 ± 0.003^{a}	0.037 ± 0.002^{a}	0.028 ± 0.001^{b}	0.031 ± 0.002^{ab}	**	**	**			*		*			
		Fine root diameter	μm	FR-Dia	404.95 ± 8.32^{a}	374.96 ± 8.15^{bc}	388.27 ± 1.95^{ab}	348.22 ± 8.61^{c}	**		**		*	***			**		
		Fine root specific root length	$m \cdot g^{-1}$	FR-SRL	288.10 ± 11.34^{a}	342.28 ± 17.57^{a}	377.10 ± 21.55^{b}	423.75 ± 23.45^{c}	**	**	**		**	***	*	***	*	*	
Anatomy	None	Fine root Ks	$kg \cdot s^{-1} \cdot m^{-1} \cdot MPa^{-1}$	FR-Ks	0.54 ± 0.07^{a}	0.63 ± 0.16^{a}	0.66 ± 0.15^{a}	0.64 ± 0.13^{a}	**				*	***					
	Passive	Leaf Ks	$kg \cdot s^{-1} \cdot m^{-1} \cdot MPa^{-1}$	LF-Ks	4.55 ± 0.45^{a}	4.27 ± 0.53^{a}	3.66 ± 0.42^{ab}	3.34 ± 0.33^{b}	**	**				***		***			L(*) to (ns)
		Stem cortex thickness	μm	ST-CTh	262.41 ± 15.68^{a}	266.45 ± 12.93^{a}	227.65 ± 11.37^{b}	225.16 ± 10.32^{b}	**	**			**	***		***			L(*) to (ns)
		Stem xylem thickness	μm	ST-XTh	314.49 ± 11.57^{a}	293.74 ± 7.17^{a}	234.98 ± 9.27^{b}	205.33 ± 8.60^{c}	**	**		*	***	***		***			L(*) & LxN(*) to (ns)
		Tap root cortex thickness	μm	TR-CTh	209.14 ± 8.67^{a}	209.20 ± 8.06^{a}	182.66 ± 13.98^{b}	186.40 ± 9.60^{ab}	**	**				***					L(*) to (ns)

TABLE 1 (Continued)

Category	Treatment response	Trait	Unit	Abbreviation	Light-Rich	Light-poor	Shade-rich	Shade-poor	w/o biomass G	L	N	L×N	Including biomass Mass	G	MxG	L	N	L×N	Change with mass
	Passive & active	Stem vascular thickness	µm	ST-VTh	651.28 ± 22.70[a]	593.58 ± 21.77[b]	479.75 ± 21.92[c]	436.78 ± 19.99[d]	**	**	**		***	***	*	**		*	N(*) to LxN(*)
		Stem Ks	kg·s⁻¹·m⁻¹·MPa⁻¹	ST-Ks	8.62 ± 0.77[a]	9.86 ± 0.89[ab]	11.12 ± 1.11[b]	9.56 ± 1.09[ab]	**	**	**	*	***	***		***	**	**	LxN(*) to N(*)
		Tap root Ks	kg·s⁻¹·m⁻¹·MPa⁻¹	TR-Ks	27.16 ± 4.14[a]	28.32 ± 4.08[a]	29.43 ± 3.84[a]	30.49 ± 4.31[a]	**					***		**			L(ns) to (*)
		Tap root stele diameter	µm	TR-SDia	888.75 ± 60.60[a]	769.73 ± 44.59[a]	569.64 ± 22.97[b]	517.38 ± 30.58[c]	**	**	**		**	***	*			*	L(*) & N(*) to LxN(*)
	Active	Leaf palisade thickness	µm	LF-PTh	141.35 ± 4.60[a]	136.74 ± 4.61[ab]	124.16 ± 3.96[bc]	122.22 ± 3.20[c]	**	**				***		*			
		Leaf spongy thickness	µm	LF-STh	79.96 ± 4.93[a]	74.11 ± 4.63[ab]	70.79 ± 2.85[b]	73.60 ± 4.85[ab]	**	*	*	*	*	***	*	**	*	*	
		Fine root cortex thickness	µm	FR-CTh	136.38 ± 2.99[a]	125.46 ± 3.58[a]	127.44 ± 4.13[a]	113.25 ± 2.07[b]	*		*			**			*		
		Fine root stele diameter	µm	FR-SDia	113.38 ± 5.27[a]	103.50 ± 4.28[b]	111.68 ± 5.01[ab]	104.40 ± 4.44[ab]	**	**	**			***			*		

Note: Rich versus poor designates high nutrients versus 10% nutrient concentration treatment. For each trait, the ANOVA effects of genotype (G), light (L) and nutrient (N) stresses, and their interactions (L × N) are presented, without (w/o) or with plant total biomass (Mass) included as a covariate: ***: $p < .001$, **: $p < .01$, *: $p < .05$. Based on the difference between the models with and without biomass as covariate, we assigned a treatment response as either passive (primarily scaling with mass), active (adjusted independent of mass), or a combination thereof. For each treatment combination, the mean ± SE of 10 genotypes (estimated marginal mean from the ANOVA, based on 5–6 replicates per genotype) is presented for each trait. Different lower-case letters represent significant ($p < .05$) Tukey's post hoc differences among treatments for each trait from the ANOVA without biomass as a covariate.

FIGURE 2 Leaf and fine root morphology across a factorial of light and nutrient limitation. Light/shade, direct sun versus 50% shade. Rich/poor, high nutrients versus 10% nutrient concentration. (a) specific leaf area (LF-SLA, cm^2 g^{-1}), (b) leaf mass fraction (LF-MF, %), (c) specific root length (FR-SRL, cm/g), (d) fine root mass fraction (FR-MF, %), (e) ratio of leaf area to root length (RatioSLA-SRL), and (f) ratio of leaf mass to fine root mass (RatioLF-FRmass). Points indicate genotype ($n = 10$) mean ($n = 5$–6) at a given treatment. Boxplots show distribution of values. Different letters represent significant ($p < .05$) Tukey's post hoc differences between treatments for each trait
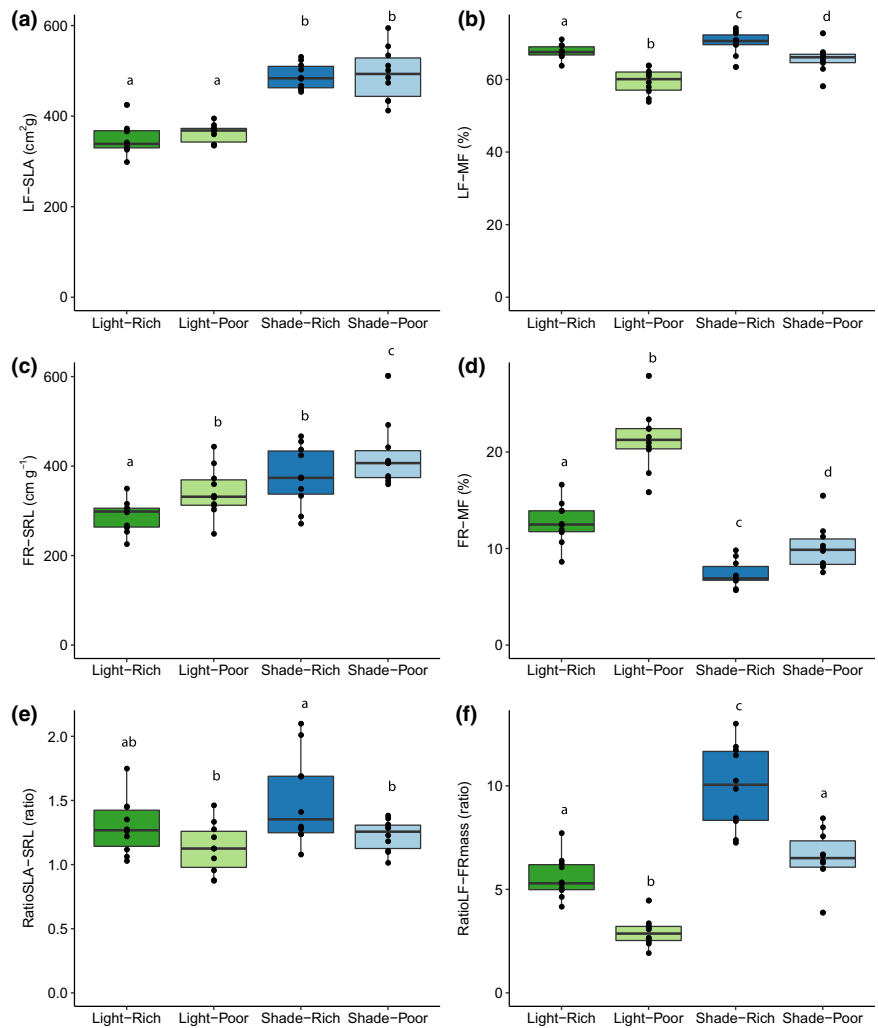
additionally considers surface area per unit mass of acquisitive organ, paralleled with that of the RatioLF-FRmass, with a trend of increasing under light limitation and decreasing under nutrient limitation (Figure 2e).

For morphological traits, light limitation affected 11 of the 12 traits, all except for FR-Dia (fine root diameter) (Table 1). The responses led to increases in acquisitive values for resource acquiring traits, such as LF-SLA (Figure 2a), FR-SRL (Figure 2c), TR-SRL (tap root-specific root length), and ST-Hgt (stem height). There were also strong decreases in organ dimensions, for example, LF-Th (leaf thickness), ST-Dia (stem diameter), and TR-Dia (tap root diameter). LF-Den (leaf density), ST-Den (stem density), and FR-Den (fine root density) also declined. Contrasting with the effect of light limitation, nutrient limitation affected only four of 12 morphological traits (Table 1), leading to decreased ST-Dia and FR-Dia, and increased FR-SRL and TR-Den (tap root density).

For anatomical traits, limiting resources affected 12 of the 13 traits, and responses again differed by limiting resource (Figure 3 and Table 1). Light limitation affected anatomical traits of all three organs. Aboveground, light limitation decreased LF-PTh (leaf palisade parenchyma layer thickness), ST-CTh (stem cortex thickness), ST-VTh (stem vascular bundle thickness), and ST-XTh (stem xylem

thickness). Belowground, light limitation decreased TR-CTh (tap root cortex thickness) and TR-SDia (tap root stele diameter). Vascular tissue adjustment to light limitation led to changes in theoretical hydraulic conductivity, with decreased LF-Ks (leaf hydraulic conductivity) but increased ST-Ks (stem hydraulic conductivity). In contrast to the effects of light limitation, nutrient limitation predominately affected fine root anatomy, leading to decreased FR-CTh (fine root cortex thickness) and FR-SDia (fine root stele diameter).

To assess the role of passive mass-based scaling in the responses of resource limitations, trait responses were reanalyzed with mass as a covariate in the model (Table 1, Figure S3), effectively comparing treatments again for trait values of plant of the same size. Contrasting the results of the two models (including mass as covariate in Table 1), we designated the observed response as being primarily passive (scaling with mass), primarily active (adjusted independent of mass-scaling), or a mixture of both (Table 1).

For six traits, the responses to resource limitation were primarily passive responses, with effects no longer evident when mass was included as covariate. This included two morphological traits (FR-Den and TR-SRL) and four anatomical traits (LF-Ks, ST-CTh, ST-XTh, and TR-CTh). For these traits, the observed response to light limitation primarily was associated with smaller plant size.
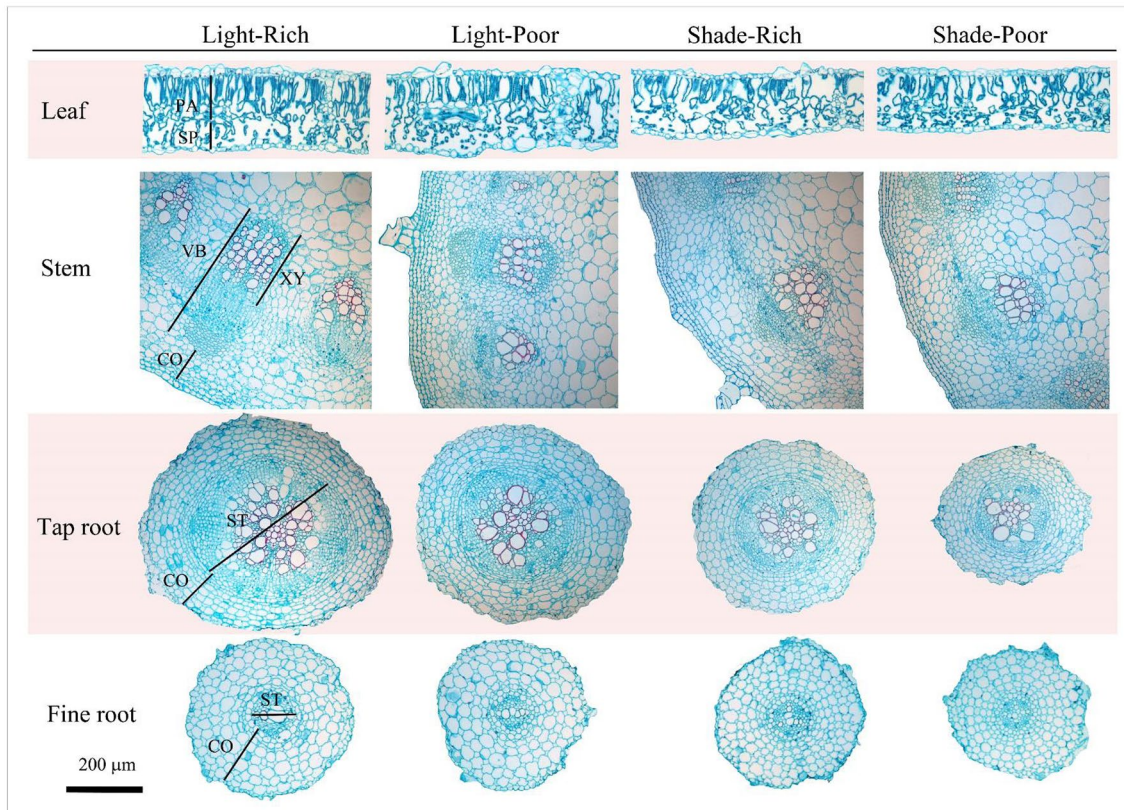
FIGURE 3 Typical anatomical structure of leaf, stem, tap root, and fine root of genotype HA across a factorial of light and nutrient limitation. Light/shade, direct sun versus 50% shade. Rich/poor, high nutrients versus 10% nutrient concentration. CO, cortex; PA, palisade tissue; SP, spongy tissue; ST, stele; VB, vascular bundle; XY, xylem

For 13 traits, the responses were primarily active, with effects not changing when mass was included in the model, indicating that the response was still evident after correcting for plant size. This included three allocational traits (ST-MF, FR-MF, and TR-MF), six morphological traits (LF-Th, LF-SLA, LF-Den, ST-Den, FR-Den, and FR-SRL), and four anatomical traits (LF-PT, LF-ST, FR-CT, and FR-*SD*). For these traits, resource limitation effects were not associated with smaller plant size.

For 11 traits, the responses were a mixture of passive and active responses to resource limitation, with the effects differed somewhat when mass was included in the model, indicating that scaling with mass accounted for a portion of the response. This included three allocational traits (LF-MF, RatioLF-FRmass, and RatioSLA-SRL), four morphological traits (ST-Dia, ST-Hgt, TR-Dia, and TR-Den), and four anatomical traits (ST-VTh, ST-Ks, TR-SDia, and TR-Ks).

3.2 | How do traits compare for magnitude of relative plasticity and what role does size scaling of traits play in this?

The magnitude and direction of trait plasticity in response to resource limitation were assessed with a RDPI (Figure 4a). The RDPI for at least one of the treatments was significantly different from control for all of the traits expect FR-Ks. Visually comparing RDPI per trait category showed that allocational traits had the greatest plastic responses, followed by morphology, and then anatomy. Although the treatment that combined light and nutrient limitation ("shade-poor" in Figure 4a) resulted in the largest decline in biomass, it was not consistently the treatment that induced the greatest magnitude of plasticity across all of the traits.

When trait responses to resource limitation were corrected for plant mass (Figure 4b), the extent to which RDPI values were affected was variable. Since this RDPI analysis is based on genotype means instead of individual plants, there are slight differences in the extent of active versus passive responses though results broadly lined up with the prior analysis (Table 1). For traits where responses were designated as primarily passive (Table 1), correcting for plant mass resulted in substantially lower RDPI (e.g., comparing RDPI in 4b to 4a for TR-SRL, LF-Ks, and ST-XT). For traits where responses were designated as primarily active, correcting for plant mass had little effect on RDPI (e.g., comparing 4b to 4a for ST-MF, FR-MF, LF-SLA, and LF-PT). For traits where responses were designated as a combination of active and passive, correcting for plant mass had a variable effect on RDPI. For some traits, RDPI was reduced for at least one treatment when mass was factored out (e.g., LF-MF, RatioLF-FRmass, and ST-Dia), indicating that the passive and active components that response were complementary in direction, resulting in a greater overall magnitude. However,
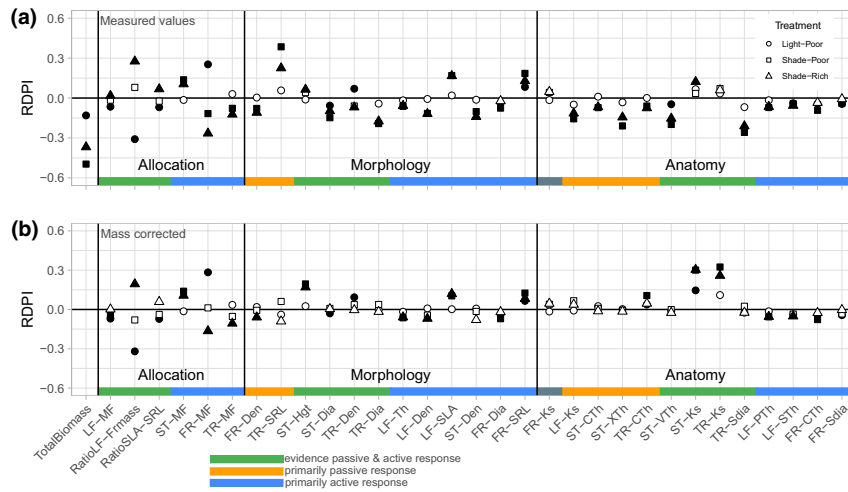
FIGURE 4 Trait plasticity in response to resource limitation. Points indicate the average (*n* = 10) relative distance plasticity index (RDPI) in response to light limitation (triangles, Shade-Rich) or nutrient limitation (circles, Light-Poor), or combined (squares, Shade-Poor). Symbol fill represents a *t* test significance (*p* < .05) of RDPI being different from zero (filled symbols) or not (open symbols). Traits are ordered based on their treatment response, primarily passive (scaling with mass), primarily active (adjusted independent of mass), or a combination thereof. (a) RDPI values taken from base measurements. (b) RDPI values when correcting trait values for biomass. Trait abbreviations as in Table 1
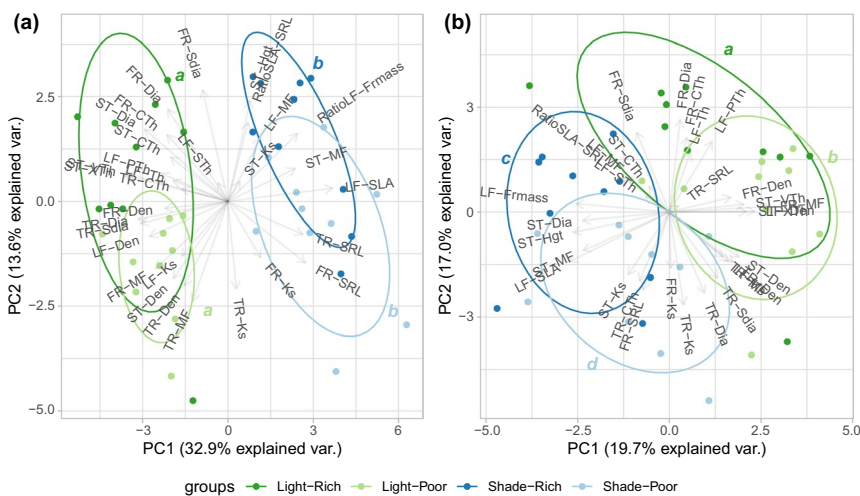
FIGURE 5 Principal component analysis (PCA) of leaf, stem, and roots traits in response to resource limitations. Light/shade, direct sun versus 50% shade. Rich/poor, high nutrients versus 10% nutrient concentration. Panels represent (a) trait values as measured, and (b) trait values after correcting for size scaling (allometric effects). Different letters indicate significant Hotelling's *t* test, after Bonferroni correction, between treatments on the first two principal components. Trait abbreviations and units as in Table 1

for a few traits, such as ST-Hgt, ST-Ks, and TR-Ks, correcting for plant mass resulted in a greater RDPI, indicating active and passive responses to be in opposite directions, or antagonistic (Figure S2).

3.3 | Do traits show a coordinated shift due to resource limitation across all organs and what role does size scaling of traits play in this?

When the genotype means for the observed traits in all three trait categories (allocation, morphology, and anatomy) and all treatments were included in a PCA, the correlations among many of the traits

become evident. PC1 and PC2 explained 34.4% and 13.4% of the variation, respectively (Figure 5a). Light limitation resulted in a shift of a key set of traits to be more acquisitive along the first axis, with higher LF-SLA, TR-SRL, and FR-SRL under shade associated with lower values of other morphological traits (LF-Den, ST-Dia, TR-Dia, and TR-SDia) and lower anatomical trait values (ST-XTh and ST-VTh). Nutrient limitation resulted in a smaller shift in traits, oriented more on PC2, and dominated by higher TR-MF, TR-Den, and TR-Ks and lower RatioSLA-SRL, ST-Hgt, FR-Dia, and FR-SDia (Figure S4).

When the trait values corrected for mass were included in a PCA, reflecting primarily active responses, the correlations among traits changed and less of the variation was explained (PC1 and PC2

explained 19.7% and 17.0% of the variation, respectively). Responses to light and nutrient limitation were more similar in scale, although still resource specific (Figure 5b). Thus, while the passive mass effect of light limitation might be greater, the active responses to above- and belowground resource limitation were similar in magnitude.

4 | DISCUSSION

Here, we assessed the direction, magnitude, and coordination of cultivated *H. annuus* responses to light or/and nutrient limitation for traits in multiple categories (allocation, morphology, and anatomy) and across all organ (leaves, stem, and roots), using plants harvested at a similar age and developmental stage. We found that more biomass was allocated to the organs acquiring the most limiting resource (roots for nutrient stress and leaves for shade), and that there were additional morphological and anatomical trait adjustments that generally led to more acquisitive trait values (e.g., higher LF-SLA in shade and higher FR-SRL in nutrient stress). We explored the role of mass-scaling in these responses by looking at the effect of including whole plant dry mass as a covariate to correct for plant size. The trait responses to resource limitations varied in the extent to which they were primarily passive (i.e., associated with lower biomass of stressed plants), primarily active (not or only marginally associated with lower biomass of stressed plants), or a combination thereof. The variable magnitude and direction of active plasticity played an appreciable role in shaping the individual trait responses and the overall coordinated response that was unique to each resource limitation.

4.1 | Allocation, morphology, and anatomy responses to above- and belowground resource limitations

Light limitation resulted in increased relative investment in aboveground plant parts and nutrient limitation resulted in increased relative investment in belowground parts, consistent with the expectation that plasticity serves to optimize/maximize the uptake of the most limiting resource (Figure 1 and Table 1) (Bloom et al., 1985; Poorter et al., 2012; Shipley & Meziane, 2002). This allocation pattern has been confirmed in other species and growth forms (e.g., grasses, Siebenkäs et al., 2015; shrubs, Valladares et al., 2000; trees, Reich et al., 1998, Poorter et al., 2012; Kramer-Walter & Laughlin, 2017). Additionally, morphological and anatomical adjustments resulted in a higher LF-SLA and FR-SRL, under light and nutrient limitation, respectively, decreasing the ratio of mass invested to resource uptake potential (Figures 2,3). Anatomical adjustments in leaf and root, such as decreased LF-PTh and FR-CTh, also reduced tissue metabolic and maintenance costs (Galindo-Castañeda et al., 2018; Guo et al., 2006; Jaramillo et al., 2013). Thus, for *H. annuus*, greater capacity for resource acquisition was coupled with reduced costs, and this was achieved by a combination of passive and active plasticity.

The traits varied in the extent to which passive plasticity played a role in explaining the observed response to resource limitations (Figure 4 and Table S2). The response to both light and nutrient limitation appeared primarily passive for several morphological and anatomical traits, but not for any of the allocational responses. And, the extent of passive adjustment differed by resource. Similar to Poorter et al., 2012, we found that responses to light limitation were more often passive than for nutrient limitation. For many traits, there was evidence of a mixture of passive and active responses, which could be complementary or antagonistic and thus influence the magnitude of the overall/observed response (Figure 4, Figure S2). However, after correcting for plant mass, treatment effects remained significant for all of the allocation traits and many morphological and anatomical traits, such as LF-SLA (Freschet et al., 2018; Reich, 2018; this study), FR-SRL, LF-PTh, and FR-CTh (this study), indicating active adjustments of these key traits for obtaining the most limited above- or belowground resource.

4.2 | Magnitude and direction of plasticity

Consistent with other resource limitation studies, the observed plasticity of mass allocational traits was largest, followed by morphological traits (Kramer-Walter & Laughlin, 2017; Valladares et al., 2000), and smallest in anatomical traits (Cai et al., 2017; Catoni et al., 2015; Xu et al., 2015). It should be noted that differences in the extent of plasticity for different categories of traits may be species specific or based on the traits included. For example, oak (*Quercus robur*) seedlings were more plastic in physiological traits under shade, yet beech (*Fagus sylvatica)* was more plastic in morphological traits (Valladares et al., 2002). Differences among trait categories for the magnitude of plasticity may reflect an inherent hierarchy originating from the internal component traits of any specific organ. For example, leaf thickness is highly correlated with palisade parenchyma (Scoffoni et al., 2015), and root diameter with cortex and/or stele thickness (Kong et al., 2014). Thus, small shifts in individual component anatomical traits could add up to larger shifts in morphological traits which in turn affect allocational traits.

For traits where there was evidence of a mixture of passive and active plasticity, the alignment of both components (i.e., complementary or antagonistic in direction) affected the direction and magnitude of the observed response (Figure 4, Figure S2). For RatioLF-FRmass, the passive and active responses to light limitation combined to enhance the relative investment in leaves, increasing the capacity for light acquisition. For other traits, correcting for mass revealed substantive active plasticity that was antagonistic to passive plasticity. For example, the active plasticity for ST-Hgt, and ST-Ks and TR-Ks was of greater magnitude than the observed response. The active adjustments counteracted the passive scaling with mass and resulted in shaded plants with higher conducting capacity (TR-Ks and ST-Ks) as well as high axial transportation distance and total transpiring surface (ST-Hgt and LF-SLA). This suggests that a coordinated increase in axial root and stem hydraulic transport offset greater resistance due to a longer transportation distance (Plavcová & Hacke, 2012), facilitating efficient

movement of carbon to roots and nutrients and water to leaves (Maurel et al., 2010; Rodríguez-Gamir et al., 2016; Wahl et al., 2001). Thus, both passive and active trait adjustments to resource limitation serve to increase resource uptake capacity and maintain (optimal) functioning of altered organs.

Where passive and active trait adjustments are antagonistic, this could indicate a departure from "safe" trait values under non-limiting conditions. For example, increased ST-Ks may come at the cost of increased risk of xylem embolism in shaded plants (Tyree & Zimmermann, 2002). The anatomical dataset collected in this work provides an excellent resource for anatomical water flow models (Couvreur et al., 2018), to further shed light on the consequences of these anatomical trait adjustments for plant hydraulics and how plants balance resource uptake demands with stress safety margins.

4.3 | Coordinated trait shifts

Resource limitation led to a coordinated shift among many correlated traits, with an overall shift toward greater potential for resource acquisition, consistent with other resource manipulation studies for commonly measured traits (Freschet et al., 2015). The coordinated trait shifts differed by limiting resource, with light limitation dominated by higher LF-SLA and associated with lower FL-Den and shifts in other stem and tap root traits, while nutrient limitation dominated by thinner FR-SDia, FR-Dia, and TR-MF and associated with other root and stem traits (Figure 5 and Table 1). Correcting traits for plant size altered the magnitude of responses and relationships among traits, and revealed that the active effects of light and nutrient limitation were still resource specific, but more similar in magnitude.

The coordinated trait plasticity in response to resource limitations was generally a resource-specific shift in traits toward more acquisitive strategy that was not evident across all organs. It is interesting to note that these patterns are not consistent with the "whole plant economic spectrum", expectation of correlated evolution of conservative traits across all organs and resource limitations (Díaz et al., 2016; Reich, 2014). This plasticity is an example of extensive responses to resource limitations and other abiotic or biotic factors that undoubtedly contribute to variation captured in broader surveys of plants specialized in different habitats (Anderegg et al., 2018). As such, these findings contribute to ongoing efforts to understand the scale dependence of trait covariation and the role that trait plasticity plays at both ecological and evolutionary scales.

5 | CONCLUSIONS

Few studies have assessed the phenotypic response of whole plants in terms of biomass allocation, organ morphology, and anatomy, simultaneously, and even less under multiple resource limitation. Here, our research demonstrates that major traits from all three categories shift in response to resource limitation. Many of these shifts are passive, that is, scaling with decreased mass of plants under stressed conditions. Moreover, these passive shifts

extend well beyond mass allocational traits and include both morphological and anatomical traits. The magnitude and direction of individual traits responses and their coordination are driven not only by passive scaling with plant mass, but by an additional active component that can be complementary or antagonistic to the effect of mass-scaling. Thus, for a full understanding of plants' response to environmental stress, both this passive and active plasticity needs to be taken into account.

AUTHOR CONTRIBUTIONS

YW, AT, and LD designed the experiment. YW carried out the experiment and took all measurements. YW and AT analyzed the results. YW wrote the initial manuscript draft with revisions by AT and LD. All authors contributed to manuscript revision, and read and approved the submitted version.

ORCID

Yan Wang https://orcid.org/0000-0003-2730-2394
Andries A. Temme https://orcid.org/0000-0001-9451-6566

REFERENCES

Agrawal, A. A. (2020). A scale-dependent framework for tradeoffs, syndromes, and specialization in organismal biology. *Ecology*, *101*, e02924. https://doi.org/10.1002/ecy.2924

Anderegg, L. D. L., Berner, L. T., Badgley, G., Sethi, M. L., Law, B. E., & HilliRisLambers, J. (2018). Within-species patterns challenge our understanding of the leaf-economics spectrum. *Ecology Letters*, *21*, 734–744. https://doi.org/10.1111/ele.12945

Bates, D., Maechler, M., Bolker, B., Christensen, R. H. B., Singmann, H., Dai, B., Scheipl, F., Grothendieck, G., & Green, P. (2018). Package 'lme4'.

Bloom, A. J., Chapin, F. S., & Mooney, H. A. (1985). Resource limitation in plants - An economic analogy. *Annual Review of Ecology and Systematics*, *16*, 363–392. https://doi.org/10.1146/annurev.es.16.110185.002051

Bowsher, A. W., Mason, C. M., Goolsby, E. W., & Donovan, L. A. (2016). Fine root tradeoffs between nitrogen concentration and xylem vessel traits precludes unified whole-plant resource strategies in *Helianthus*. *Ecology and Evolution*, *6*, 1016–1031.

Bowsher, A. W., Shelby, K. C., Ahmed, I., Krall, E., Reagan, D. J., Najdowski, M. N., & Donovan, L. A. (2017). Genotype Rankings for Nutrient Stress Resistance are Unrelated to Stress Severity in Cultivated Sunflower (*Helianthus annuus* L.). *Journal of Agronomy and Crop Science*, *203*, 241–253.

Cai, Q., Ji, C., Yan, Z., Jiang, X., & Fang, J. (2017). Anatomical responses of leaf and stem of *Arabidopsis thaliana* to nitrogen and phosphorus addition. *Journal of Plant Research*, *130*, 1035–1045. https://doi.org/10.1007/s10265-017-0960-2

Catoni, R., Gratani, L., Sartori, F., Varone, L., & Granata, M. U. (2015). Carbon gain optimization in five broadleaf deciduous trees in

response to light variation within the crown: Correlations among morphological, anatomical and physiological leaf traits. *Acta Botanica Croatica*, *74*, 71–94. https://doi.org/10.1515/botcro-2015-0010

Chatelet, D. S., Clement, W. L., Sack, L., Donoghue, M. J., & Edwards, E. J. (2013). The evolution of photosynthetic anatomy in *Viburnum* (Adoxaceae). *International Journal of Plant Sciences*, *174*, 1277–1291.

Couvreur, V., Faget, M., Lobet, G., Javaux, M., Chaumont, F., & Draye, X. (2018). Going with the flow: Multiscale insights into the composite nature of water transport in roots. *Plant Physiology*, *178*, 1689–1703. https://doi.org/10.1104/pp.18.01006

Díaz, S., Kattge, J., Cornelissen, J. H. C., Wright, I. J., Lavorel, S., Dray, S., Reu, B., Kleyer, M., Wirth, C., Colin Prentice, I., Garnier, E., Bönisch, G., Westoby, M., Poorter, H., Reich, P. B., Moles, A. T., Dickie, J., Gillison, A. N., Zanne, A. E., … Gorné, L. D. (2016). The global spectrum of plant form and function. *Nature*, *529*, 167–171. https://doi.org/10.1038/nature16489

Donovan, L. A., Mason, C. M., Bowsher, A. W., Goolsby, E. W., & Ishibashi, C. D. A. (2014). Ecological and evolutionary lability of plant traits affecting carbon and nutrient cycling. *Journal of Ecology*, *102*, 302–314. https://doi.org/10.1111/1365-2745.12193

Eissenstat, D. M., & Achor, D. S. (1999). Anatomical characteristics of roots of citrus rootstocks that vary in specific root length. *New Phytologist*, *141*, 309–321. https://doi.org/10.1046/j.1469-8137.1999.00342.x

Fortunel, C., Fine, P. V. A., & Baraloto, C. (2012). Leaf, stem and root tissue strategies across 758 Neotropical tree species. *Functional Ecology*, *26*, 1153–1161. https://doi.org/10.1111/j.1365-2435.2012.02020.x

Fox, J., Weisberg, S., Price, B., Adler, D., Bates, D., Baud-Bovy, G., Bolker, B., Ellison, S., Firth, D., Friendly, M., Gorjanc, G., Graves, S., Heriberger, R., & Laboissiere, R. (2018) Package 'car'.

Freschet, G. T., Swart, E. M., & Cornelissen, J. H. C. (2015). Integrated plant phenotypic responses to contrasting above- and below-ground resources: Key roles of specific leaf area and root mass fraction. *New Phytologist*, *206*, 1247–1260. https://doi.org/10.1111/nph.13352

Freschet, G. T., Violle, C., Bourget, M. Y., Scherer-Lorenzen, M., & Fort, F. (2018). Allocation, morphology, physiology, architecture: The multiple facets of plant above- and below-ground responses to resource stress. *New Phytologist*, *219*, 1338–1352. https://doi.org/10.1111/nph.15225

Galindo-Castañeda, T., Brown, K. M., & Lynch, J. P. (2018). Reduced root cortical burden improves growth and grain yield under low phosphorus availability in maize. *Plant, Cell & Environment*, *41*, 1579–1592. https://doi.org/10.1111/pce.13197

Gedroc, J., McConnaughay, K. D. M., & Coleman, J. S. (1996). Plasticity in root/shoot partitioning: Optimal, ontogenetic, or both? *Functional Ecology*, *1*, 44–50. https://doi.org/10.2307/2390260

Gu, J., Xu, Y., Dong, X., Wang, H., & Wang, Z. (2014). Root diameter variations explained by anatomy and phylogeny of 50 tropical and temperate tree species. *Tree Physiology*, *34*, 415–425. https://doi.org/10.1093/treephys/tpu019

Guo, D., Xia, M., Wei, X., Chang, W., Liu, Y., & Wang, Z. (2008). Anatomical traits associated with absorption and mycorrhizal colonization are linked to root branch order in twenty-three Chinese temperate tree species. *New Phytologist*, *180*, 673–683. https://doi.org/10.1111/j.1469-8137.2008.02573.x

Guo, X. R., Cao, K. F., & Xu, Z. F. (2006). Acclimation to irradiance in seedlings of three tropical rain forest Garcinia species after simulated gap formation. *Photosynthetica*, *44*, 193–201. https://doi.org/10.1007/s11099-006-0006-9

Jaramillo, R. E., Nord, E. A., Chimungu, J. G., Brown, K. M., & Lynch, J. P. (2013). Root cortical burden influences drought tolerance in maize. *Annals of Botany*, *112*, 429–437. https://doi.org/10.1093/aob/mct069

John, G. P., Scoffoni, C., Buckley, T. N., Villar, R., Poorter, H., & Sack, L. (2017). The anatomical and compositional basis of leaf mass per area. *Ecology Letters*, *20*, 412–425. https://doi.org/10.1111/ele.12739

Kong, D., Ma, C., Zhang, Q., Li, L., Chen, X., Zeng, H., & Guo, D. (2014). Leading dimensions in absorptive root trait variation across 96 subtropical forest species. *New Phytologist*, *203*, 863–872. https://doi.org/10.1111/nph.12842

Kramer-Walter, K. R., Bellingham, P. J., Millar, T. R., Smissen, R. D., Richardson, S. J., & Laughlin, D. C. (2016). Root traits are multidimensional: Specific root length is independent from root tissue density and the plant economic spectrum. *Journal of Ecology*, *104*, 1299–1310. https://doi.org/10.1111/1365-2745.12562

Kramer-Walter, K. R., & Laughlin, D. C. (2017). Root nutrient concentration and biomass allocation are more plastic than morphological traits in response to nutrient limitation. *Plant and Soil*, *416*, 539–550. https://doi.org/10.1007/s11104-017-3234-9

Lenth, R., Singmann, H., Love, J., Buerkner, P., Herve, M., & Abd Allah, E. F. (2018). Package 'emmeans'.

Mandel, J. R., Dechaine, J. M., Marek, L. F., & Burke, J. M. (2011). Genetic diversity and population structure in cultivated sunflower and a comparison to its wild progenitor, *Helianthus annuus* L. *Theoretical and Applied Genetics*, *123*, 693–704. https://doi.org/10.1007/s00122-011-1619-3

Masalia, R. R., Temme, A. A., Torralba, N. D. L., & Burke, J. M. (2018). Multiple genomic regions influence root morphology and seedling growth in cultivated sunflower (*Helianthus annuus* L.) under well-watered and water-limited conditions. *PLoS One*, *13*, e204279.

Mason, C. M., & Donovan, L. A. (2015). Evolution of the leaf economic spectrum in herbs: Evidence from environmental divergences in leaf physiology across *Helianthus*. *Evolution*, *69*, 2705–2720.

Maurel, C., Simonneau, T., & Sutka, M. (2010). The significance of roots as hydraulic rheostats. *Journal of Experimental Botany*, *61*, 3191–3198. https://doi.org/10.1093/jxb/erq150

McConnaughay, K. D. M., & Coleman, J. S. (1999). Biomass allocation in plants: Ontogeny or optimality a test along three resource gradients. *Ecology*, *8*, 2581–2593. https://doi.org/10.1890/0012-9658(1999)080[2581:BAIPOO]2.0.CO;2

McElrone, A. J., Pockman, W. T., Martínez-Vilalta, J., & Jackson, R. B. (2004). Variation in xylem structure and function in stems and roots of trees to 20 m depth. *New Phytologist*, *163*, 507–517. https://doi.org/10.1111/j.1469-8137.2004.01127.x

Medeiros, J. S., Burns, J. H., Nicolson, J., Roger, L., & Valverde-Barrantes, O. (2017). Decoupled leaf and root carbon economics is a key in the ecological diversity and evolutionary divergence of deciduous and evergreen lineages of genus *Rhododendron*. *American Journal of Botany*, *104*, 803–816.

Muir, C. D., Conesa, M. A., Roldán, E. J., Molins, A., & Galmés, J. (2017). Weak coordination between leaf structure and function among closely related tomato species. *New Phytologist*, *213*, 1642–1653. https://doi.org/10.1111/nph.14285

Nambeesan, S. U., Mandel, J. R., Bowers, J. E., Marek, L. F., Ebert, D., Corbi, J., Rieseberg, L. H., Knapp, S. J., & Burke, J. M. (2015). Association mapping in sunflower (*Helianthus annuus* L.) reveals independent control of apical vs. basal branching. *BMC Plant Biology*, *15*, 84.

Nicotra, A. B., Atkin, O. K., Bonser, S. P., Davidson, A. M., Finnegan, E. J., Mathesius, U., Poot, P., Purugganan, M. D., Richards, C. L., Valladares, F., & van Kleunen, M. (2010). Plant phenotypic plasticity in a changing climate. *Trends in Plant Science*, *15*, 684–692. https://doi.org/10.1016/j.tplants.2010.09.008

Osnas, J. L. D., Lichstein, J. W., Reich, P. B., & Pacala, S. W. (2013). Global leaf trait relationships: Mass, area, and the leaf economics spectrum. *Science*, *340*, 741–744. https://doi.org/10.1126/science.1231574

Pilote, A. J., & Donovan, L. A. (2016). Evidence of correlated evolution and adaptive differentiation of stem and elf functional traits in the herbaceous genus, *Helianthus*. *American Journal of Botany*, *103*, 2096–2114.

Plavcová, L., & Hacke, U. G. (2012). Phenotypic and developmental plasticity of xylem in hybrid poplar saplings subjected to experimental drought, nitrogen fertilization, and shading. *Journal of Experimental Botany*, *18*, 6481–6491. https://doi.org/10.1093/jxb/ers303

Poorter, H., Niinemets, Ü., Ntagkas, N., Siebenkäs, A., Mäenpää, M., Matsubara, S., & Pons, T. L. (2019). A meta-analysis of plant responses to light intensity for 70 traits ranging from molecules to whole plant performance. *New Phytologist*, *223*, 1073–1105. https://doi.org/10.1111/nph.15754

Poorter, H., Niklas, K. J., Reich, P. B., Oleksyn, J., Poot, P., & Mommer, L. (2012). Biomass allocation to leaves, stems and roots: Meta-analyses of interspecific variation and environmental control. *New Phytologist*, *193*, 30–50. https://doi.org/10.1111/j.1469-8137.2011.03952.x

Reich, P. B. (2014). The world-wide 'fast-slow' plant economics spectrum: A traits manifesto. *Journal of Ecology*, *102*, 275–301. https://doi.org/10.1111/1365-2745.12211

Reich, P. B. (2018). Do plants increase resource acquisition potential in the face of resource shortfalls, and if so, how? *New Phytologist*, *219*, 1142–1144. https://doi.org/10.1111/nph.15363

Reich, P. B., Tjoelker, M. G., Walters, M. B., Vanderklein, D. W., & Bushena, C. (1998). Close association of RGR, leaf and root morphology, seed mass and shade tolerance in seedlings of nine boreal tree species grown in high and low light. *Functional Ecology*, *12*, 327–338. https://doi.org/10.1046/j.1365-2435.1998.00208.x

Rice, S. A., & Bazzaz, F. A. (1989). Quantification of plasticity of plant traits in response to light intensity - comparing phenotypes at a common weight. *Oecologia*, *78*, 502–507. https://doi.org/10.1007/BF00378741

Rico, C., Pitterman, J., Polley, H. W., Aspinwell, M. J., & Fay, P. A. (2013). The effect of subambient to elevated CO_2 concentration on vascular function in *Helianthus annuus*: Implications for plant response to climate change. *New Phytologist*, *199*, 956–965.

Rodríguez-Gamir, J., Primo-Millo, E., & Forner-Giner, M. Á. (2016). An integrated view of whole-tree hydraulic architecture. Does stomatal or hydraulic conductance determine whole tree transpiration? *PLoS One*, *11*, e155246.

Ryser, P., & Eek, L. (2000). Consequences of phenotypic plasticity vs. interspecific differences in leaf and root traits for acquisition of aboveground and belowground resources. *American Journal of Botany*, *3*, 402–411. https://doi.org/10.2307/2656636

Scoffoni, C., Kunkle, J., Pasquet-Kok, J., Vuong, C., Patel, A. J., Montgomery, R. A., Givnish, T. J., & Sack, L. (2015). Light-induced plasticity in leaf hydraulics, venation, anatomy, and gas exchange in ecologically diverse Hawaiian lobeliads. *New Phytologist*, *207*, 43–58. https://doi.org/10.1111/nph.13346

Shipley, B., & Meziane, D. (2002). The balanced-growth hypothesis and the allometry of leaf and root biomass allocation. *Functional Ecology*, *16*, 326–331. https://doi.org/10.1046/j.1365-2435.2002.00626.x

Siebenkäs, A., Schumacher, J., & Roscher, C. (2015). Phenotypic plasticity to light and nutrient availability alters functional trait ranking across eight perennial grassland species. *AoB Plants*, *7*, plv029. https://doi.org/10.1093/aobpla/plv029

Sperry, J. S., Hacke, U. G., & Pittermann, J. (2006). Size and function in conifer tracheids and angiosperm vessels. *American Journal of Botany*, *93*, 1490–1500.

Sugiura, D., & Tateno, M. (2011). Optimal leaf-to-root ratio and leaf nitrogen content determined by light and nitrogen availabilities. *PLoS One*, *6*, e22236. https://doi.org/10.1371/journal.pone.0022236

Temme, A. A., Kerr, K. L., & Donovan, L. A. (2019). Vigour/tolerance trade-off in cultivated sunflower (*Helianthus annuus*) response to

salinity stress is linked to lead elemental composition. *Journal of Agronomy and Crop Science*, *205*, 508–518.

Tyree, M. T., & Ewers, F. W. (1991). The hydraulic architecture of trees and other woody plants. *New Phytologist*, *119*, 345–360. https://doi.org/10.1111/j.1469-8137.1991.tb00035.x

Tyree, M. T., & Zimmermann, M. H. (2002). *Xylem structure and the ascent of sap*. Springer.

Valladares, F., Chico, J., Aranda, I., Balaguer, L., Dizengremel, P., Manrique, E., & Dreyer, E. (2002). The greater seedling high-light tolerance of *Quercus robur* over *Fagus sylvatica* is linked to a greater physiological plasticity. *Trees*, *16*, 395–403. https://doi.org/10.1007/s00468-002-0184-4

Valladares, F., Gianoli, E., & Gómez, J. M. (2007). Ecological limits to plant phenotypic plasticity. *New Phytologist*, *176*, 749–763. https://doi.org/10.1111/j.1469-8137.2007.02275.x

Valladares, F., Sanchez-Gomez, D., & Zavala, M. A. (2006). Quantitative estimation of phenotypic plasticity: Bridging the gap between the evolutionary concept and its ecological applications. *Journal of Ecology*, *94*, 1103–1116. https://doi.org/10.1111/j.1365-2745.2006.01176.x

Valladares, F., Wright, S. J., Lasso, E., Kitajima, K., & Pearcy, R. W. (2000). Plastic phenotypic response to light of 16 congeneric shrubs from a Panamanian rainforest. *Ecology*, *81*, 1925–1936. https://doi.org/10.1890/0012-9658(2000)081[1925:PPRTLO]2.0.CO;2

Van Kleunen, M., & Fisher, M. (2005). Constraints on the evolution of adaptive phenotypic plasticity in plants. *New Phytologist*, *166*, 49–60. https://doi.org/10.1111/j.1469-8137.2004.01296.x

Wahl, S., Ryser, P., & Edwards, P. (2001). Phenotypic plasticity of grass root anatomy in response to light intensity and nutrient supply. *Annals of Botany*, *88*, 1071–1078. https://doi.org/10.1006/anbo.2001.1551

Weiner, J. (2004). Allocation, plasticity and allometry in plants. *Perspectives in Plant Ecology, Evolution and Systematics*, *6*, 207–215. https://doi.org/10.1078/1433-8319-00083

Wickham, H., Chang, W., Henry, L., Pederson, T. L., Takahashi, K., Wikle, C., & Woo, K. (2018). Package 'ggplot2'.

Wilson, P. J., Thompson, K., & Hodgson, J. G. (1999). Specific leaf area and leaf dry matter content as alternative predictors of plant strategies. *New Phytologist*, *143*, 155–162. https://doi.org/10.1046/j.1469-8137.1999.00427.x

Wright, I. J., Reich, P. B., Westoby, M., Ackerly, D. D., Baruch, Z., Bongers, F., Cavender-Bares, J., Chapin, T., Cornelissen, J. H. C., Diemer, M., Flexas, J., Garnier, E., Groom, P. K., Gulias, J., Hikosaka, K., Lamont, B. B., Lee, T., Lee, W., Lusk, C., … Villar, R. (2004). The worldwide leaf economics spectrum. *Nature*, *428*, 821–827. https://doi.org/10.1038/nature02403

Xu, N., Wang, R., Liu, J., Lu, P., & Guo, W. (2015). Hierarchy of plasticity traits in responses of *Quercus aliena* to light conditions and water availability. *Dendrobiology*, *74*, 169–180. https://doi.org/10.12657/denbio.074.017

SUPPORTING INFORMATION

Additional supporting information may be found online in the Supporting Information section.